

# Generation of highly nonclassical $n$ -photon polarization states by superbunching at a photon bottleneck

Holger F. Hofmann\*

*PRESTO, Japan Science and Technology Corporation (JST), Research Institute for Electronic Science, Hokkaido University, Kita-12 Nishi-6, Kita-ku, Sapporo 060-0812, Japan*

(Received 27 November 2003; revised manuscript received 26 May 2004; published 24 August 2004)

It is shown that coherent superpositions of two oppositely polarized  $n$ -photon states can be created by postselecting the transmission of  $n$  independently generated photons into a single-mode transmission line. It is thus possible to generate highly nonclassical  $n$ -photon polarization states using only the bunching effects associated with the bosonic nature of photons. The effects of mode-matching errors are discussed and the possibility of creating  $n$ -photon entanglement by redistributing the photons into  $n$  separate modes is considered.

DOI: 10.1103/PhysRevA.70.023812

PACS number(s): 42.50.Dv, 03.67.Mn, 42.50.Ar

## I. INTRODUCTION

The creation of highly nonclassical states is one of the fundamental challenges in quantum optics. In particular, multiphoton entanglement and superpositions of macroscopically distinguishable states (commonly referred to as cat states, after Schrödinger's famous cat paradox [1]) may be very useful as resources for optical quantum-information processes such as teleportation, cloning, or quantum computation [2–7]. Recently, it has been shown that multiphoton entanglement can indeed be created and manipulated using only single-photon sources, beam splitters, and postselection based on precise photon detection [8–15]. In previous investigations, these methods have been applied to photonic qubits, where the goal was to obtain exactly one photon per spatial mode. In order to achieve this kind of output, it is necessary to discard the cases where several photons bunch up in a single spatial mode as unwanted errors. However, it is also possible to specifically select cases where several photons bunch up in the same mode. In particular, this method has been used to propose the generation of spatial mode entanglement [16,17].

In the following, a related proposal is presented for the generation of highly nonclassical polarization states. It is shown that a coherent superposition of two oppositely polarized  $n$ -photon polarization states can be obtained by transmitting  $n$  independently generated photons with homogeneously distributed polarizations into a single spatial mode. For large photon numbers, this  $n$ -photon polarization state has the nonclassical statistical properties of a cat state, since the superposition is between two well separated regions of the Poincaré sphere [18] and the two polarization states can be distinguished by measuring only a few photons. On the other hand, highly nonclassical interference effects between the two components of the superposition will be observable in the polarization statistics of the Stokes vector components

orthogonal to the polarization along which the superposition is prepared [19].

Once a cat-state superposition of polarization states is realized in a single mode, it is also possible to generate the corresponding multiparticle entangled state by redistributing the photons into separate channels, effectively transforming the local state of  $n$  photons in one spatial mode into an entangled state of  $n$  photons in  $n$  spatial modes. In the present proposal, the photons are then transferred from  $n$  input modes to  $n$  output modes through a single-mode bottleneck. The quantum interference effects associated with the bosonic nature of photons leads to a superbunching effect in the polarization, resulting in maximal  $n$ -photon entanglement in the output. It is thus possible to realize a strong interaction between an arbitrarily large number of photons by temporarily bunching them into a single-mode channel. The superbunching effect at a photon bottleneck may therefore be a useful tool in the realization of a wide range of multiphoton quantum operations.

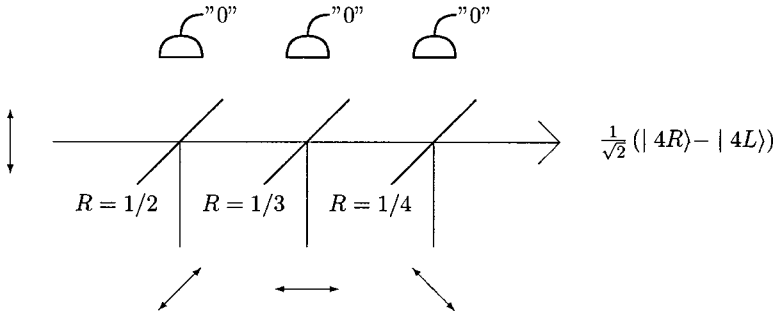
## II. THE SUPERBUNCHING EFFECT

The bunching effect used to obtain the nonclassical polarization state can be understood by considering the analogy with two-photon bunching. If a horizontally polarized photon and a vertically polarized photon are transmitted into the same spatial mode, their circular polarizations will always be the same—either both right polarized or both left polarized. Quantum interference removes the component with different circular polarization. This effect can be generalized to  $n$  photons by choosing a homogeneous distribution of linear polarization angles. The quantum interference between the different linear single-photon polarizations then removes all components of the circular polarization, except for the two components where all photons have the same circular polarization. However, quantum coherence between the two maximally polarized cases is preserved since the bunching effect does not distinguish between right or left circular polarization.

The validity of this argument can be verified by defining the following  $n$ -photon input state:

---

\*Present address: Graduate School of Advanced Sciences of Matter, Hiroshima University, Kagamiyama 1-3-1, Higashi Hiroshima 739-8530, Japan. Electronic address: h.hofmann@osa.org



$$|\psi_{\text{in}}\rangle = 2^{-(n/2)} \prod_{l=0}^{n-1} \left[ \hat{a}_R^\dagger(l) + \exp\left(-i\frac{2\pi}{n}l\right) \hat{a}_L^\dagger(l) \right] |\text{vac}\rangle, \quad (1)$$

where  $\hat{a}_R^\dagger(l)$  and  $\hat{a}_L^\dagger(l)$  are the creation operators of right and left circular polarization in the spatial mode  $l$ . The rotation of the linear polarization in the input ports  $l$  is thus represented by the phases of  $2\pi l/n$  in the superposition of the circular polarization components. Linear optics can then be used to transfer all  $n$  input modes into a single-mode output port described by

$$\begin{aligned} \hat{b}_R &= \frac{1}{\sqrt{n}} \sum_{l=0}^{n-1} \hat{a}_R(l), \\ \hat{b}_L &= \frac{1}{\sqrt{n}} \sum_{l=0}^{n-1} \hat{a}_L(l). \end{aligned} \quad (2)$$

Each input mode  $\hat{a}_{R/L}(l)$  thus contributes equally to the correspondingly polarized output mode  $\hat{b}_{R/L}$ . Photon losses to output modes other than  $\hat{b}_{R/L}$  can be avoided by postselection using high-quantum-efficiency photon detectors in all unused output ports. If any photon losses are detected, the output is discarded. This postselection procedure can then be represented by a projection operator  $\hat{P}$ . The non-normalized postselected output state then reads

$$|\psi_{\text{out}}\rangle = \hat{P}|\psi_{\text{in}}\rangle = (2n)^{-n/2} \prod_{l=0}^{n-1} \left[ \hat{b}_R^\dagger + \exp\left(-i\frac{2\pi}{n}l\right) \hat{b}_L^\dagger \right] |\text{vac}\rangle. \quad (3)$$

Since the postselection condition represented by  $\hat{P}$  has made the photons from different input ports indistinguishable in the output, the terms with the same overall number of right and left circular polarized photons now interfere with each other. Because all sums over varying phase factors  $\exp[-i2\pi l/n]$  are zero, the only two remaining terms in the output are the component with only right circular polarized photons and the component with only left circular polarized photons,

$$\begin{aligned} |\psi_{\text{out}}\rangle &= (2n)^{-n/2} \{ (\hat{b}_R^\dagger)^n + \exp[-i\pi(n-1)] (\hat{b}_L^\dagger)^n \} |\text{vac}\rangle \\ &= \sqrt{\frac{n!}{(2n)^n}} [ |n;0\rangle - (-1)^n |0;n\rangle ], \end{aligned} \quad (4)$$

where the final result is expressed in the photon number ba-

FIG. 1. Schematic setup for the generation of a four-photon-polarization cat state. Each input port receives one-photon with the linear polarization indicated above. The detectors ensure that no photons are emitted into the empty output ports, and the beam splitter reflectivities are chosen so that each input component has equal weight in the output.

sis of the right and left circular polarization modes in the output. Note that the elimination of all other components of circular polarization can also be justified by a symmetry argument. Since the distribution of input polarizations has an  $n$ -fold symmetry with respect to rotations of the Stokes vector around the circular polarization axis [or a  $(2n)$ -fold rotation symmetry of the linear polarization], and since the operations applied are not sensitive to the polarization at all, the output state must also have this  $n$ -fold symmetry. However, any coherent superposition of the maximally polarized states  $|n;0\rangle$  and  $|0;n\rangle$  with other polarization states would reduce this symmetry [19]. Therefore, the cat-state superposition of  $|n;0\rangle$  and  $|0;n\rangle$  is the only possible output state that preserves the  $n$ -fold symmetry of the input.

In postselection methods, the difficulty of generating highly nonclassical states is directly reflected in the probability of obtaining the postselection condition that indicates a successful generation of the target state. In the present case, this condition is given by the probability that no photons are detected in any spatial modes other than the output modes  $\hat{b}_{R/L}$ . The probability of success for this postselection procedure is given by

$$p(n) = \langle \psi_{\text{out}} | \psi_{\text{out}} \rangle = \frac{2n!}{(2n)^n}. \quad (5)$$

Since the probability of finding all photons in the same spatial output mode rapidly decreases with increasing photon number, the efficiency of generating highly nonclassical superpositions is very low. However, the probability of success is still significantly higher than the probability of finding all of  $n$  independent particles in the output channel. For example, the probability of finding three photons in the output is  $p(3) = 1/18$ . For three independent particles, the chance of finding all three in the output channel would be only  $(1/3)^3 = 1/27$ . This enhancement of the postselection probability increases with increasing photon number and may thus be helpful in the suppression of errors caused by imperfect mode matching between the input photons (see below).

Figure 1 shows an example of an optical setup to generate a cat-state superposition of four-photon polarization. The cascade setup shown can easily be generalized to arbitrary photon numbers. Each input photon is generated by a single photon source with a well defined linear polarization, as indicated in the figure. The postselection condition is that no photons are detected in the three detectors set up at the empty output ports. Note that it would also be sufficient to postselect the arrival of all four photons at detectors in the

output. This may be useful to avoid errors due to the limited quantum efficiencies of the detectors, although it might restrict the possibilities of further quantum operations on the output.

### III. POLARIZATION STATISTICS OF THE OUTPUT STATE

The polarization statistics of the output can be characterized by the Stokes parameters, defined as the photon number difference between a pair of orthogonal polarizations. The properties of the quantized Stokes parameters then correspond to the properties of the spin components of a spin- $n/2$  system [19]. The quantum statistics of four-photon polarization thus corresponds to a spin-2 system, and the five possible photon distributions between any two orthogonal polarizations correspond to the five eigenvalues of the respective spin component.

The most impressive feature of the superbunching effect is the accumulation of all photons in the two states with maximal circular polarization, given by the circular polarization statistics  $p_{RL}(n_R, n_L)$ ,

$$\begin{aligned} p_{RL}(4;0) &= 1/2, \\ p_{RL}(3;1) &= 0, \\ p_{RL}(2;2) &= 0, \\ p_{RL}(1;3) &= 0, \\ p_{RL}(0;4) &= 1/2. \end{aligned} \quad (6)$$

However, the observation of this bunching effect around  $n_R - n_L = \pm 4$  does not indicate coherence between the two components. To distinguish the quantum superposition from a statistical mixture, it is necessary to consider the linear polarization statistics. These can be obtained from the coherent overlap of the two components  $|4R\rangle$  and  $|4L\rangle$  with the basis states of a linear polarization measurement rotated by an angle of  $\phi$  relative to the horizontal and vertical polarization axes, where the individual basis states are defined by the photon number difference  $\Delta n(\phi)$  between the two orthogonal polarizations,

$$\begin{aligned} \langle \Delta n = +4 | 4R \rangle &= 1/4 \exp[-i4\phi], \\ \langle \Delta n = +4 | 4L \rangle &= 1/4 \exp[+i4\phi], \\ \langle \Delta n = +2 | 4R \rangle &= 1/2 \exp[-i4\phi], \\ \langle \Delta n = +2 | 4L \rangle &= -1/2 \exp[+i4\phi], \\ \langle \Delta n = 0 | 4R \rangle &= \sqrt{6}/4 \exp[-i4\phi], \\ \langle \Delta n = 0 | 4L \rangle &= \sqrt{6}/4 \exp[+i4\phi], \\ \langle \Delta n = -2 | 4R \rangle &= 1/2 \exp[-i4\phi], \end{aligned}$$

$$\begin{aligned} \langle \Delta n = -2 | 4L \rangle &= -1/2 \exp[+i4\phi], \\ \langle \Delta n = -4 | 4R \rangle &= 1/4 \exp[-i4\phi], \\ \langle \Delta n = -4 | 4L \rangle &= 1/4 \exp[+i4\phi]. \end{aligned} \quad (7)$$

As the linear polarization is rotated, the interference terms in the photon number distribution thus oscillate with a periodicity of  $8\phi$ ,

$$\begin{aligned} p_\phi(+4) &= \frac{1}{16}(1 - \cos[8\phi]), \\ p_\phi(+2) &= \frac{4}{16}(1 + \cos[8\phi]), \\ p_\phi(0) &= \frac{6}{16}(1 - \cos[8\phi]), \\ p_\phi(-2) &= \frac{4}{16}(1 + \cos[8\phi]), \\ p_\phi(-4) &= \frac{1}{16}(1 - \cos[8\phi]). \end{aligned} \quad (8)$$

Figure 2 shows the characteristic polarization statistics of the superbunched superposition state. Figure 2(a) shows the superbunching effect in the circular polarization statistics; Figs. 2(b) to 2(d) show the linear polarization statistics for polarization angles of  $\phi=0$ ,  $\phi=\pi/8$ , and  $\phi=\pi/16$ , respectively. Note that the polarization angles are defined relative to the four input polarizations, that is, the sensitivity of the output statistics to the linear polarization direction originates from the anisotropy caused by the selection of a particular set of input polarizations. Specifically, the polarization statistics of linear polarizations that coincide with one of the input polarizations ( $\phi=0$  and  $\phi=\pi/4$ ) always have exactly three photons in one polarization and one in the other [ $\Delta n(\phi) = \pm 2$ ], as can be seen in Fig. 2(b). This distribution of photons can be understood as a combination of the preservation of the input polarization (one input photon in each of the two observed output polarizations) and the conventional bunching effect between the remaining two photons, which adds exactly two photons to either one of the two output polarizations. On the other hand, the polarization statistics of linear polarizations that are exactly halfway between two of the input polarizations ( $\phi=\pi/8$  and  $\phi=3\pi/8$ ) are clearly dominated by the 75% probability of finding equal numbers of photons in both polarizations [ $\Delta n(\phi)=0$ ], as can be seen in Fig. 2(d). In this case, the complete absence of photon distributions with  $\Delta n(\phi) = \pm 2$  indicates a strong quantum interference effect between the circular polarization components. The linear polarization statistics that would also be expected for the maximally right or left polarized states  $|4R\rangle$  or  $|4L\rangle$  are obtained at angles of  $\phi=\pi/16$ ,  $\phi=3\pi/16$ , etc., as shown in Fig. 2(c). These statistics correspond to the binomial distribution expected if each photon had a random linear polarization. The deviations from this binomial distribution thus show that the

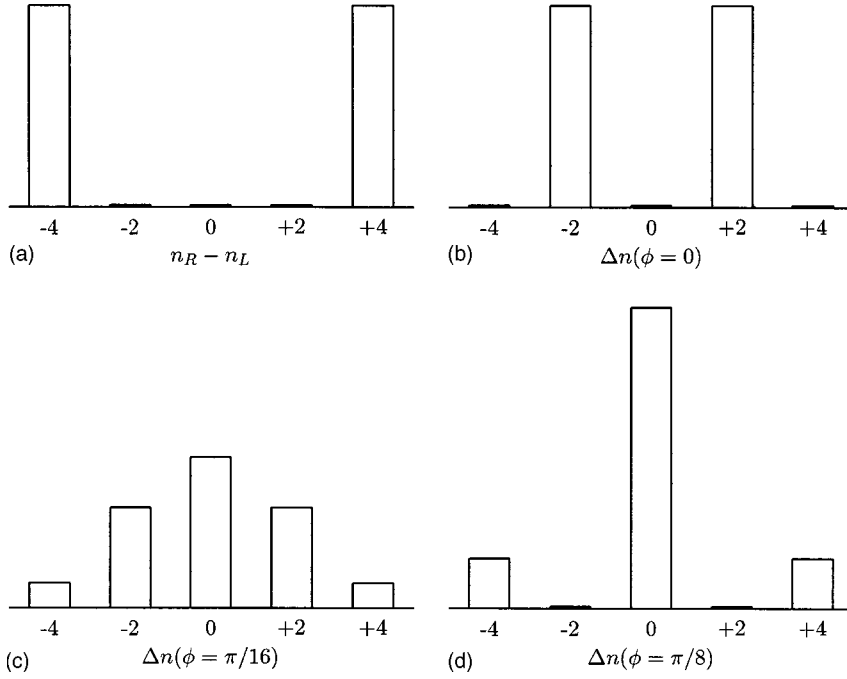


FIG. 2. Illustration of the characteristic polarization statistics of a superposition state of the two four-photon states with maximal circular polarization  $|4R\rangle$  and  $|4L\rangle$ . (a) shows the circular polarization statistics, (b) shows the linear polarization statistics along the horizontal and vertical directions ( $\phi=0$ ), (c) shows the polarization statistics at an angle of  $\pi/16$  relative to the horizontal and vertical directions, and (d) shows the polarization statistics at an angle of  $\pi/8$ . Note that the linear polarization statistics have a periodicity of  $\pi/4$ , that is, the statistics shown in (a) also applies to an angle of  $\pi/4$ , etc.

polarization statistics cannot be explained in terms of a simple combination of individual photon polarizations.

#### IV. EFFECTS OF MODE-MATCHING ERRORS

Experimentally, the superbunching effect requires that all input photons can be matched into the same mode at the beam splitters. Therefore, the most likely source of errors is an imperfect mode matching at one of the input ports. Since the effect of such errors is quite different from the decoherence effects normally expected in spin systems, it may be of interest to investigate the polarization statistics associated with a mode-matching error in more detail.

The characteristics of a mode-matching error can be obtained by assuming that one of the photons is in a different mode from the other three. The output polarization state is then a product state of a three-photon state with modified bunching effects and a single-photon state with the unchanged input polarization. If the mismatched photon is horizontally polarized [represented by the contribution with  $l=0$  in Eq. (1)], the output state of the remaining three photons is given by

$$\begin{aligned} & \frac{1}{16\sqrt{2}}(\hat{a}_R^\dagger + i\hat{a}_L^\dagger)(\hat{a}_R^\dagger - \hat{a}_L^\dagger)(\hat{a}_R^\dagger - i\hat{a}_L^\dagger)|\text{vac}\rangle \\ &= \frac{\sqrt{3}}{16}|3;0\rangle - \frac{1}{16}|2;1\rangle + \frac{1}{16}|1;2\rangle - \frac{\sqrt{3}}{16}|0;3\rangle. \end{aligned} \quad (9)$$

Note that the circular polarization statistics of this state is independent of the linear polarization of the mismatched photon. Therefore, all mode-matching errors modify the circular polarization in the same way. However, the loss of symmetry will be apparent in the linear polarization statistics.

The total output state is obtained as a product state of the bunched three-photon state given by Eq. (9) and the single

horizontally polarized photon transmitted to the output port with a probability of  $1/4$ . In the circular polarization basis, this product state of three-photon and one-photon polarization in the output reads

$$\begin{aligned} |\psi_{3\otimes 1}\rangle &= \frac{1}{32\sqrt{2}}(\sqrt{3}|3;0\rangle - |2;1\rangle + |1;2\rangle - \sqrt{3}|0;3\rangle) \otimes (|1;0\rangle \\ &+ |0;1\rangle). \end{aligned} \quad (10)$$

The total amplitude of this state describes the postselection probability. It is interesting to compare this probability to the perfectly mode-matched four-photon postselection probability  $p(4)$ ,

$$\langle \psi_{3\otimes 1} | \psi_{3\otimes 1} \rangle = \frac{1}{128} = \frac{2}{3}p(4). \quad (11)$$

The mode mismatch thus reduces the postselection probability for the four photons from  $3/256$  to  $2/256$ . Experimentally, this dependence of successful postselection on mode matching could be observed by varying the delay time of one of the input photons, thus varying the phase matching artificially [20]. It is then possible to evaluate the mode matching from the rates of coincidence counts obtained in the experiment.

The statistics of circular polarization obtained from a single-photon mismatch error corresponding to the output state  $|\psi_{3\otimes 1}\rangle$  reads

$$p_{3\otimes 1}(4;0) = \frac{3}{16},$$

$$p_{3\otimes 1}(3;1) = \frac{4}{16},$$

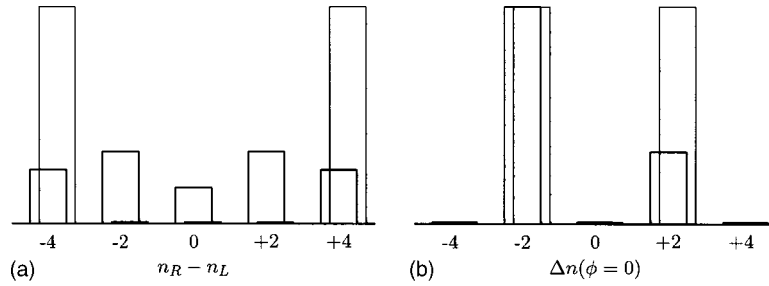


FIG. 3. Illustration of the change in the polarization statistics caused by a one-photon mode-matching error. (a) shows the circular and (b) shows the horizontal and vertical polarization statistics. The thick lines show the polarization statistics of the error component, corresponding to three photons in the same mode and one photon in a different mode, as given by Eqs. (10) and (13). The thin lines show the output probabilities for the ideal four-photon bunching. The difference in the total probability corresponds to the change of postselection probability.

$$\begin{aligned}
 p_{3\otimes 1}(2;2) &= \frac{2}{16}, \\
 p_{3\otimes 1}(1;3) &= \frac{4}{16}, \\
 p_{3\otimes 1}(0;4) &= \frac{3}{16}.
 \end{aligned}
 \tag{12}$$

This distribution sharply contrasts with the bunching effect of the perfectly mode-matched case given by Eq. (6). The main effect of the mode-matching error is thus to destroy the bunching effect, while the coherence between the circularly polarized components, which corresponds to the linear polarization statistics, is affected much less.

To evaluate the effects of the mode mismatch on the linear polarization components, it is useful to transform the output state into the horizontal and vertical basis states ( $\phi = 0$ ). In this basis, the state reads

$$|\psi_{3\otimes 1}\rangle = \frac{1}{16\sqrt{2}}(\sqrt{3}|3V\rangle - |2H;1V\rangle) \otimes |1H\rangle.
 \tag{13}$$

The horizontal and vertical polarization statistics thus still includes only the two components with  $\Delta n = \pm 2$ , corresponding to three photons in one polarization and one in the other. The only change compared to the statistics for  $\phi = 0$  given in Eq. (8) is that the vertically polarized output is preferred.

Figure 3 shows a comparison of the polarization statistics for the one-photon mode mismatch with the perfectly mode-matched four-photon output. Note that the changed postselection probability has been taken into account, so that the

sum over all probabilities shown is 1.5 times higher for the perfectly mode-matched case. Most importantly, mode-matching errors have more impact on the circular polarization statistics than on the linear polarization statistics which depends on coherence between the circular polarization eigenstates. The errors expected in the generation of a superposition state of  $|4R\rangle$  and  $|4L\rangle$  by superbunching are therefore quite different from the decoherence effects normally associated with cat-state superpositions. In the case of a small mode-matching error probability  $\epsilon$ , the expected circular polarization distribution can be derived by mixing the ideal distribution of Eq. (6) with the error distribution given in Eq. (12). Taking the different postselection probabilities into account, this distribution is given by

$$\begin{aligned}
 p_{\text{error}}(n;4-n) &= \frac{3}{256}(1-\epsilon)p_{RL}(n;4-n) \\
 &+ \frac{1}{128}\epsilon p_{3\otimes 1}(n;4-n).
 \end{aligned}
 \tag{14}$$

It is thus possible to estimate the mode-matching error from the experimental data obtained in measurements of the circular polarization output.

**V. GENERATION OF MULTIPARTICLE ENTANGLEMENT**

Once a highly nonclassical  $n$ -photon polarization state is generated in a single mode, this state can be converted into an  $n$ -particle entangled state by distributing the photons into

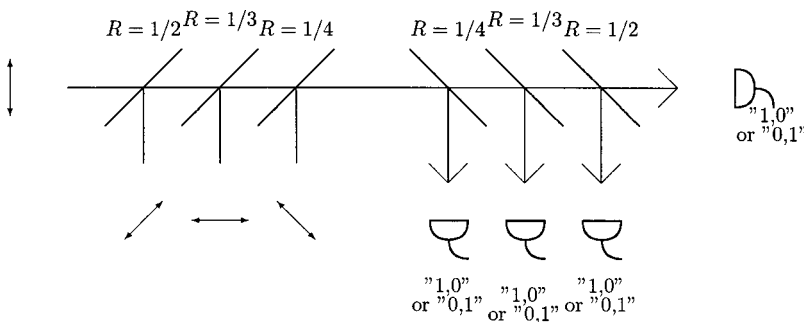


FIG. 4. Schematic setup for the generation of multiparticle entanglement using the photon bottleneck. In this case, postselection by polarization-sensitive detection in the four output channels is necessary to redistribute the photons into different modes.



$n$  separate channels. It is then possible to apply the criteria for entanglement verification to quantify the nonclassical features of the polarization statistics. Figure 4 illustrates a possible setup for the generation of four-photon entanglement using a photon bottleneck. In this setup, it is necessary to post select the output by detecting exactly one-photon in each output channel using polarization-sensitive detectors. The redistribution of the photons into separate channels thus makes the output condition symmetric to the input condition and the operation of the photon bottleneck can be interpreted as a collective four-photon interaction. In the absence of errors, the output state of this interaction is the Greenberger-Horne-Zeilinger (GHZ) state,

$$|\text{GHZ}\rangle = \frac{1}{\sqrt{2}}(|RRRR\rangle - |LLLL\rangle). \quad (15)$$

Such four-photon GHZ states have recently been generated by using entangled pairs generated in downconversion as input [21–23]. The photon bottleneck provides an alternative method of generating the same type of multiparticle entanglement from previously unentangled input photons.

The analysis of mode-matching errors given above can now be applied to determine the condition for successful entanglement generation. Genuine  $n$ -particle entanglement can be satisfied by the condition [24]

$$\frac{\langle \text{GHZ} | \hat{\rho}_{\text{out}} | \text{GHZ} \rangle}{\text{Tr}\{\hat{\rho}_{\text{out}}\}} \geq \frac{1}{2}. \quad (16)$$

Using the results of Eqs. (10) and (11), it is possible to quantify the reduction in multiparticle entanglement caused by a mode-matching error as follows:

$$\frac{|\langle \text{GHZ} | \psi_{3\otimes 1} \rangle|^2}{\langle \psi_{3\otimes 1} | \psi_{3\otimes 1} \rangle} = \frac{3}{8}. \quad (17)$$

The overall reduction for small mode-matching error probabilities  $\epsilon$  can then be determined using the different postselection probabilities as

$$\frac{\langle \text{GHZ} | \hat{\rho}_{\text{out}} | \text{GHZ} \rangle}{\text{Tr}\{\hat{\rho}_{\text{out}}\}} = \frac{12 - 9\epsilon}{12 - 4\epsilon} \approx 1 - \frac{5}{12}\epsilon. \quad (18)$$

For example, even if each of the four input channels contributes a mode-matching error of 5%, for a total error probability of about 20% ( $\epsilon \approx 0.2$ ), the GHZ contribution would be reduced by only about 8.3%. The generation of multiparticle entanglement using a photon bottleneck thus appears to be very robust against typical mode-matching errors.

## VI. CONCLUSIONS

In conclusion, it has been shown that a highly nonclassical superposition state of oppositely polarized  $n$ -photon states can be generated by postselecting the transmission of  $n$  independently generated photons into a single spatial mode. No initial entanglement is needed, and the postselection conditions require only zero detection events. In principle, the method can be applied to any number of photons. It can be used to generate catlike superpositions in the polarization statistics of single-mode  $n$ -photon states, or to obtain GHZ-type  $n$ -photon entanglement. The error analysis suggests that the nonclassical correlations that can be generated by this method are sufficiently robust with regard to experimental imperfections. The photon bottleneck setup presented in this paper may therefore provide a useful tool for the generation and control of nonclassical states of light.

- 
- [1] E. Schrödinger, *Naturwissenschaften* **23**, 807 (1935); **23**, 823 (1935); **23**, 844 (1935); reprint of the English translation in *Quantum Theory and Measurement*, edited by J. A. Wheeler and W. H. Zurek (Princeton University Press, Princeton, NJ, 1983), pp. 3–49, 138–141.
- [2] M. Muraio, M. B. Plenio, and V. Vedral, *Phys. Rev. A* **61**, 032311 (2000).
- [3] P. van Loock and S. L. Braunstein, *Phys. Rev. Lett.* **84**, 3482 (2000).
- [4] M. Muraio, D. Jonathan, M. B. Plenio, and V. Vedral, *Phys. Rev. A* **59**, 156 (1999).
- [5] D. Gottesmann and I. L. Chuang, *Nature (London)* **402**, 390 (1999).
- [6] T. C. Ralph, A. Gilchrist, G. J. Milburn, W. J. Munro, and S. Glancy, *Phys. Rev. A* **68**, 042319 (2003).
- [7] S. D. Bartlett and W. J. Munro, *Phys. Rev. Lett.* **90**, 117901 (2003).
- [8] E. Knill, R. Laflamme, and G. Milburn, *Nature (London)* **409**, 46 (2001).
- [9] T. C. Ralph, A. G. White, W. J. Munro, and G. J. Milburn, *Phys. Rev. A* **65**, 012314 (2002).
- [10] H. F. Hofmann and S. Takeuchi, *Phys. Rev. A* **66**, 024308 (2002).
- [11] T. C. Ralph, N. K. Langford, T. B. Bell, and A. G. White, *Phys. Rev. A* **65**, 062324 (2002).
- [12] T. B. Pittman, M. J. Fitch, B. C. Jacobs, and J. D. Franson, *Phys. Rev. A* **68**, 032316 (2003).
- [13] H. F. Hofmann and S. Takeuchi, *Phys. Rev. Lett.* **88**, 147901 (2002).
- [14] X. B. Zou, K. Pahlke, and W. Mathis, *Phys. Rev. A* **66**, 064302 (2002).
- [15] J. Fiurasek, S. Massar, and N. J. Cerf, *Phys. Rev. A* **68**, 042325 (2003).
- [16] P. Kok, H. Lee, and J. P. Dowling, *Phys. Rev. A* **65**, 052104 (2002).
- [17] J. Fiurasek, *Phys. Rev. A* **65**, 053818 (2002).
- [18] A. Luis, *Phys. Rev. A* **66**, 013806 (2002).
- [19] H. F. Hofmann and S. Takeuchi, *Phys. Rev. A* **69**, 042108 (2004).
- [20] K. Sanaka, T. Jennewein, J.-W. Pan, K. Resch, and A. Zeilinger, *Phys. Rev. Lett.* **92**, 017902 (2004).
- [21] J.-W. Pan, M. Daniell, S. Gasparoni, G. Weihs, and A.

- Zeilinger, Phys. Rev. Lett. **86**, 4435 (2001).
- [22] M. Eibl, S. Gaertner, M. Bourennane, C. Kurtsiefer, M. Zukowski, and H. Weinfurter, Phys. Rev. Lett. **90**, 200403 (2003).
- [23] Z. Zhao, T. Yang, Y.-A. Chen, A.-N. Zhang, M. Zukowski, and J.-W. Pan, Phys. Rev. Lett. **91**, 180401 (2003).
- [24] O. Gühne, P. Hyllus, D. Bruß, A. Ekert, M. Lewenstein, C. Macchiavello, and A. Sanpera, J. Mod. Opt. **50**, 1079 (2003).